

DOE/BC/14126-9

(DE89000757)

NUCLEATION AND PORE GEOMETRY EFFECTS IN
CAPILLARY DESORPTION PROCESSES IN POROUS MEDIA

Topical Report

By

Mehmet Parlak

Yanis C. Yortsos

August 1989

Performed Under Contract No. FG19-87BC14126

University of Southern California

Los Angeles, California

Bartlesville Project Office
U. S. DEPARTMENT OF ENERGY
Bartlesville, Oklahoma



This report has been reproduced directly from the best available copy.

Available to DOE and DOE contractors from the Office Of Scientific and Technical Information, P.O. Box 62, Oak Ridge, TN 37831; prices available from (615)576-8401, FTS 626-8401.

Available to the public from the National Technical Information Service, U.S. Department of Commerce, 5285 Port Royal Rd., Springfield, VA 22161

Price: Printed A03
Microfiche A01

**NUCLEATION AND PORE GEOMETRY EFFECTS IN
CAPILLARY DESORPTION PROCESSES IN POROUS MEDIA**

Topical Report

By
Mehmet Parlak
Yanis C. Yortsos

August 1989

Work Performed Under Contract No. FG19-87BC14126

Prepared for
U. S. Department of Energy
Assistant Secretary for Fossil Energy

Thomas B. Reid, Project Manager
Bartlesville Project Office
P. O. Box 1398
Bartlesville, OK 74005

Prepared by
University of Southern California
Department of Petroleum Engineering
Los Angeles, CA 90089-1211

TABLE OF CONTENTS

	PAGE
Abstract.....	1
Introduction.....	2
Effects of Nucleation.....	5
Arbitrary Size Distributions.....	19
Discussion.....	25
Summary.....	30
References.....	32

FIGURES

Figure 1. Schematic of a Nucleation Site in a Pore Body..	34
Figure 2. Nucleation in a "Hydrophobic Site".....	35
Figure 3. Accessible Fraction of Bonds as a Function of Allowed Fraction p for Various Values of $f_p : Z=4$	36
Figure 4. Accessible Fraction of Sites as a Function of Allowed Fraction q for Various Values of $f_q : Z=4$	37
Figure 5. Accessible Fraction of Sites as a Function of Allowed Fraction p for Various Values of $f_q : Z=4$	38
Figure 6. Effect of Coordination Number on Limiting Site Size Distribution.....	39
Figure 7. Accessible Fraction of Sites as a Function of Allowed Fraction p for Various Values of q_i : Arbitrary Size Distributions, $Z=4$, $f_q=0$	40
Figure 8. Model Prediction of Primary Desorption for Sorption of Nitrogen for Various Values of f_q	41
Figure 9. Model Prediction of Primary Desorption for Sorption of Nitrogen for Various Values of β	42
Figure 10. Model Prediction of Secondary Desorption for Sorption of Nitrogen : $Z=4$, $f_q=0$	42
Figure 11. Model Prediction of Secondary Desorption for Sorption of Nitrogen ($q=1-(1-p)^5$): $Z=4$, $f_q=0$	43

NUCLEATION AND PORE GEOMETRY EFFECTS
IN CAPILLARY DESORPTION PROCESSES IN POROUS MEDIA

By

M. Parlak and Y.C. Yortsos

ABSTRACT

A percolation model previously developed by the authors for adsorption-desorption phenomena in porous solids (J. Colloid Interface Sci. 124, 162 (1988)), is extended to include nucleation effects during desorption, and to general size distributions of pore bodies and pore throats. Conditions under which nucleation is likely to be important are delineated. For such cases, desorption is treated as a growth problem with continuous generation of source sites. Accessibility functions are derived for Bethe lattice representations of the porous medium. Similar calculations are presented for the case when pore bodies and pore throats take arbitrary size distributions. The latter find also applications to other related processes in porous media. In view of the theory presented, the interpretation of experimental sorption isotherms is further discussed.

1. INTRODUCTION

Experimental vapor sorption isotherms are indispensable means for the characterization of the texture of porous solids (2-5). The commonly used approach relies on Kelvin's equation for the description of capillary condensation and evaporation, and on a model representation of the actual pore geometry and topology. Owing to its obvious significance, the latter has attracted considerable attention.

Early works made use of the simple model of a bundle of parallel capillaries. Such models have limited success, since they neglect connectivity and topological issues by emphasizing only local (single pore) phenomena (6-7). It is now accepted that capillary evaporation in a pore depends, in addition, to its accessibility to other vapor-occupied pores or to the bulk phase outside. The resulting hysteresis cannot be captured by local effects alone, and, as pointed out by Everett (5), requires the interplay of pore space topology.

Network models possess suitable connectivity properties and they have emerged as useful alternatives. Although their relevance to porous media was known for some time (8), successful applications to sorption processes did not start until relatively recently (9). Key realization was the similarity of features between primary desorption and ordinary percolation. Elements from the latter (10, 11) were utilized by Wall and Brown (9) to describe the hysteresis of primary sorption isotherms. Various deviations from the sharp onset of percolation were attributed to finite size effects.

Mason (12) in a detailed network study, later recognized as a percolation model on a Bethe lattice (13, 14), successfully predicted several characteristics of primary and secondary processes. Percolation concepts were also applied by Neimark (15) for primary desorption on regular lattices. A comprehensive approach outlining the relevance of percolation theory in the description of primary and secondary sorption processes was recently developed by the authors (1). Although regular lattices were also examined, Bethe lattices were exploited to obtain exact solutions. Results in (1) generalized previous expressions derived by Fisher and Essam (16) and Flory (17) to arbitrary (non-zero) fraction of initial source sites. In a concurrent study, Mason (14) revised his previous model (12), likewise pursuing a percolation approach that lead to results similar, although not identical, to those in (1).

All previous network and percolation models for capillary sorption rely on two important premises: The neglect of nucleation phenomena in the liquid-to-vapor transition, and the postulate of some form of a relationship between site and bond size distributions. Moreover, local hysteresis is tacitly assumed negligible.

Lack of nucleation attributes percolation-like features to primary desorption. It appears to have been partly justified in some experiments on porous glass (18-21), and for a variety of adsorptives. The experimental results of Barrett et al (22) on the silica-gel/nitrogen system also reveal a similar behavior. On the other hand, deviations from a percolation behavior have also been noted and variously attributed to nucleation, finite size,

vapor compressibility or other effects. At present, a quantitative assessment of the importance of nucleation during desorption is lacking.

A similar uncertainty exists in the interrelation between pore body and pore throat sizes. This issue is common to any models of porous media, and of particular interest to processes involving two phases, where occupied throats determine phase conductivity, while occupied bodies the phase volume. To be sure, any such relationship would be material-specific, reflecting the particular history (diagenetic, etc.) of the porous medium. With few exceptions, most studies bypass the issue by considering site only or bond only processes. In the mixed bond-site problem in (1) use was made of an algebraic relationship proposed in (12) to relate site and bond size distributions. This relationship is the lower limit of a general inequality reflecting the constraint that a pore body has size greater than its associated pore throats. The model developed in (1) relies exclusively on this limiting condition, thus unduly prohibiting the consideration of largely arbitrary site and bond distributions.

In this paper, these two issues are explored in some detail. Conditions to estimate nucleation effects in desorption are outlined, and simple models for nucleation during desorption are presented. The previous expressions are also generalized to account for arbitrary site and bond size distributions. The approach taken entails the special case of Zhdanov et al [23], where all bonds have the size of the associated site reduced by a constant factor. The local hysteresis in the adsorption-

desorption cycle of cylindrical elements is also briefly discussed.

Capillary sorption, by virtue of the phase change involved, may be the prototypical process, among many others involving immiscible phases (e.g. mercury porosimetry), for the direct application of percolation theory to porous media. This process is further coupled here with a nucleation mechanism that leads to accessibility-controlled growth from internal sources. Besides its direct physical relevance, the ensuing analysis may thus be useful to other percolation processes as well. Phase change in porous media is common to many applied processes (e.g. vapor-liquid flow in oil and geothermal reservoirs (24, 25)), which stand to benefit directly from the present investigation.

The paper is organized as follows: In Section 2, we briefly review the previous model and present an analysis of nucleation effects for single component systems. Section 3 deals with arbitrary site and bond size distributions. As in (1) three different problems are discussed: Bond percolation, site percolation, and a mixed problem where the accessibility of sites in bond percolation is analysed. Exact expressions valid for Bethe lattices are derived. Related implications are discussed in Section 4.

2. EFFECTS OF NUCLEATION

Before proceeding, we briefly summarize the postulates of the present model (1). The porous medium is represented by a network of bonds and sites (throats and bodies) of size distributions $\alpha_b(r)$ and $\alpha_s(r)$, and of coordination number Z .

sites and bonds have approximately spherical and cylindrical shapes, respectively, although nucleation pits on rough surfaces are also allowed (see below). Aside from this, other issues of roughness, notably those of fractal structure of the surface (26, 27), are not considered. Additional assumptions are that each pore unit (body or throat) is occupied by a single phase only, vapor or liquid, and that volumetric contributions are obtained from sites only, unless otherwise noted. Stability considerations (6) require that, if a throat is occupied by vapor (as in desorption), the adjacent two bodies are also occupied by vapor, while if a body is occupied by liquid (as in adsorption), all emanating throats are also occupied by liquid. For convenience, surface adsorption effects (28-30) are ignored.

Given a pore element (site or bond) of size r , there is a corresponding value of the relative pressure (P_V/P_{V0}) given by Kelvin's equation:

$$r = -r_{ch} / \ln(P_V/P_{V0}) \quad [11]$$

with the characteristic radius r_{ch} defined by

$$r_{ch} = 2 s \sigma V_L / (R T) \quad [12]$$

Here, σ is the surface tension, V_L the liquid molar volume, R the gas constant and T the absolute temperature, while P_V and P_{V0} are equilibrium and saturation vapor pressures, respectively.

The parameter s is geometry dependent: In sites, for both adsorption and desorption, it takes the value 1. By contrast, in the cylindrical geometry bonds, s changes from 1 for desorption to 1/2 for adsorption. This difference reflects local hysteresis for elements of cylindrical geometry, and it is tacitly assumed negligible (12-14). In the case of a single pore (infinite

connectivity), the above define the relative pressure for phase change in the element of size r . One may then parametrize the process by a variable radius, denoted hereafter for consistency (1,25,31,32) by r_d , and obtained from [11]-[21] by taking $s=1$.

Capillary adsorption (whether primary or secondary) is independent of accessibility or nucleation effects, although it may be subject to local hysteresis. At any stage r_d , vapor in all sites with $r < r_d$ and all bonds with $r < r_d/2$ is allowed to condense. However, all bonds emanating from a liquid-occupied site (size $r < r_d$) would also condense, in view of the stability considerations outlined above. Thus, a substantially larger fraction of bonds would be occupied by liquid, and the effect of geometry during adsorption would be greatly minimized. In fact, if the volumetric contribution of bonds is taken to be negligible, as in the analysis below, local geometry has no effect on the primary hysteresis loop. By contrast, local hysteresis would affect secondary desorption, where bond statistics are of primary concern. For lack of space, however, we shall postpone further discussion of this interesting case to a future study.

Desorption, on the other hand, depends strongly on accessibility and, possibly, on nucleation (heterogeneous being the most likely mechanism). In the absence of the latter, vapor occupancy during primary desorption occurs solely through access to the outside bulk vapor, first established at the percolation threshold. In secondary desorption, the liquid-to-vapor transition originates also from preexisting vapor sites.

Furthermore, when nucleation is in effect, vapor occupancy will also take place in liquid-occupied pores that are not necessarily connected to a vapor site. In the general case, therefore, the following two conditions must simultaneously hold, for an element to be occupied by vapor:

1. The pore (site or bond) is allowed to desorb, $r > r_d$.
2. The pore (site or bond) has access to
 - (a) the bulk vapor outside, and/or to
 - (b) vapor-occupied pore elements acting as internal sources. The latter may have been either present initially (e.g. in secondary desorption) or may be generated through nucleation during the process (whether primary or secondary).

Clearly, if nucleation is allowed, the formation of an infinite cluster is not required for a primary desorption process to initiate and proceed. In fact, percolation characteristics could very well be erased from the desorption isotherms. To assess their importance, the two nucleation mechanisms are separately discussed.

(i) Homogeneous Nucleation

Existing models for nucleation rates in single-component systems make use of kinetic expressions of the form (3,33-35)

$$J = K \exp\left[\frac{-4\pi\sigma r_c^2}{3kT}\right] \phi \quad [3]$$

where k is the Boltzmann constant, K is a kinetic parameter (34), and r_c is the radius of critical size nuclei related to pressure via Kelvin's equation [1]. The dimensionless function ϕ represents effects of wettability and nucleation site geometry. Its value lies between zero and one, to cover the range between perfectly heterogeneous to homogeneous nucleation. Further details can be found in (36).

Usually, the onset of nucleation is arbitrarily defined at the rate $J=1$ nucleus/sec-cc. The precise definition is immaterial, since both the critical size and the corresponding supersaturation are insensitive to large variations in J . For example, for xenon at 151 °K, an increase in J by eight orders of magnitude (from 10^{-4} to 10^{+4}) reduces the nucleation radius r_N ,

$$r_N = \{-\ln(J/K)/[(4\pi\sigma/3kT)*\phi]\}^{1/2} \quad [4]$$

from 15.4 to 13.8 Angstrom, clearly a negligible change. It follows that a quite sharp and fixed threshold for the onset of nucleation can be identified. Therefore, and without loss, J will be assumed to be unity (34,35) in subsequent examples.

When $r_d > r_N$ (vapor pressure greater than nucleation pressure), no phase change occurs via homogeneous nucleation, while when $r_d < r_N$, there is vapor occupancy via homogeneous nucleation in all pore elements (bonds and sites) of radius $r > r_d$. We recall that in the absence of nucleation, the onset of primary desorption is at the percolation threshold, defined in terms of a radius r_{pt}

$$\int_{r_{pt}}^{\infty} \alpha_b(r) dr = 1/(Z-1) \quad [5]$$

for a Bethe lattice. Note that the bond size distribution is used, since desorption is controlled by pore throats, in view of the stability premises outlined above. Thus, whether nucleation is a significant factor in a desorption experiment or not, largely depends on the ratio r_N/r_{pt} . Nucleation would be clearly negligible if the latter is significantly smaller than one.

Quantitative estimates are possible if $\alpha_b(r)$ is relatively

smooth. For Z not too large, it can be easily shown that r_{pt} is of the same order as the mean throat size λ_b . For example, for the size distribution

$$\alpha_b(r) = (\pi r / 2\lambda_b^2) \exp\{-\pi r^2 / 4\lambda_b^2\} \quad [6a]$$

we have

$$r_{pt} / \lambda_b = [4 \ln(Z-1) / \pi]^{1/2} \quad [6b]$$

the RHS of which is close to one for typical values of Z. Thus, for all practical purposes, the ratio

$$r_N / \lambda_b = [3kT \ln K / 4\pi\sigma]^{1/2} / \lambda_b \quad [7]$$

may serve to measure the importance of homogeneous nucleation. An insignificant contribution is expected for media of larger mean size, a likely occurrence in many applications.

On the other hand, sorption experiments are of utility insofar as the corresponding isotherms are not too steep, so that reasonable resolutions are possible. In turn, this requires smaller pore sizes. For instance, the slope of the sorption isotherm in a (liquid volume) vs. (relative pressure) plot is roughly equal to

$$dS_L / d(P_V / P_{V0}) \sim \alpha_s(r) r^2 \exp\{r_{ch} / r\} / r_{ch} \quad [8]$$

if equal volume sites are assumed. For a distribution of the type [6a] with an average site radius λ_s , the slope has an estimate of order λ_s / r_{ch} , near the onset of desorption. Similar conclusions are reached if it is required that the relative pressure at the onset of desorption is not too close to one. For example, a value equal to 0.8 requires $\lambda_b / r_{ch} (\sim r_{pt} / r_{ch}) \sim 4.48$.

It follows that successful sorption experiments ought to be conducted under conditions such that at the same time, λ_b / r_{ch} is not too large, and λ_b / r_N is not too small. The two requirements

are favored at higher values of σ and lower values of T , conditions commonly practiced in desorption experiments. Percolation-type theories that do not account for homogeneous nucleation, may then be successfully used for the determination of the size distributions. It can be shown that this is likely the case in typical experiments. For example, for the conditions in (18) and (21), the radii r_N and r_{ch} for xenon (water) are 14.6 (10.8) Angstrom and 13.2 (10.3) Angstrom, respectively. The corresponding porous media used have a mean pore size in the desired range. Indeed, the relative pressure for nucleation is 0.406 (0.385), while experimentally observed desorption thresholds are approximately at 0.525 (0.670). These data clearly suggest that at the onset of nucleation, most of the pore elements are already vapor-occupied via percolation mechanisms free of homogeneous nucleation.

(ii) Heterogeneous Nucleation

While homogeneous nucleation can be adequately estimated, this is hardly the case for the heterogeneous case, due to the uncertainty in the state of wettability and the geometry of the nucleation sites. Specific models or a probabilistic approach may then be necessary. Typically, the surface roughness is approximated by conical pits of the type studied by Ward et al (35) and Forest (37). Geometric and interfacial properties of the latter may further be assigned a probability distribution function.

To be specific, consider a nucleation site of conical pit geometry in a pore element (pore body) of size r (Figure 1). The

pit would be characterized by a half-width W , an angle α and a contact angle θ . Clearly, we must require that the conical pit be considerably smaller than the pore element itself, thus we take the ratio

$$\beta = W/r \quad [9]$$

to be constant and relatively small (e.g. $\beta=0.1$), for α not too small. One is then interested in determining the relative pressure (radius) at which the pore element becomes fully occupied by vapor via heterogeneous nucleation, and the corresponding effects on the desorption curve.

Closely paralleling the analysis in (35), (37) it can be shown (36) that under favorable wettability conditions (high contact angle), vapor bubbles do indeed form in the pits, possibly at a relative pressure even above that corresponding to the pore element. However, as long as the radius r_d associated with the prevailing vapor pressure is greater than the half-width W , such bubbles are restricted near the pit mouth and would grow to a generally small size with the meniscus located near the pit mouth.

Figure 2a shows a qualitative schematic of the relationship between vapor-liquid meniscus radius (r) and bubble volume (V) for a "hydrophobic" conical cavity ($\theta-\alpha < \pi/2$) satisfying the inequality $\beta < \cos(\theta-\alpha)$. The meniscus exhibits successively a local maximum ($W/\cos(\theta-\alpha)$, point A), a local minimum (W , point B), and a global maximum (r_s =site radius, point C), where the entire site becomes occupied by vapor, to be followed by an eventual reduction in radius to that of the associated bonds (point D).

From such diagrams, the stability of the equilibrium states may be readily identified (36). As with the case of homogeneous nucleation, however, and for all practical purposes, kinetic considerations would prevail in determining the occurrence of vapor occupancy.

The corresponding relationship between the change in the Helmholtz free energy ΔF and the bubble volume V is qualitatively shown in Figure 2b, for the most interesting case $W/\cos(\theta-\alpha) > r_d > W$. Two energy barriers exist. If a bubble forms with volume greater than that corresponding to the first barrier (ΔF_1), it would grow to a metastable state at the pit mouth. However, for the occupancy of the host pore element by such a bubble, a second energy barrier (ΔF_2) must be overcome, the kinetics of which are favorable only if $r_d < W$ (36). Thus, the pore may become vapor-occupied via heterogeneous nucleation, although at a relative pressure P_V^*/P_{V0} , which is considerably smaller than that of the pore element itself, P_V/P_{V0}

$$P_V^*/P_{V0} = (P_V/P_{V0})^{1/\beta} \quad [10]$$

Since β is assumed to be small, heterogeneous nucleation is, thus, likely to be important only in larger pore sizes, hence in porous media with wide size distributions and long tails (such that P_V/P_{V0} can be close to unity). It is worth noting that, at least for such model porous media, heterogeneous nucleation is pore size-hence relative pressure-dependent, in contrast to the homogeneous case.

The simplest model to be considered contains pits in each site with a constant β (half-width W is fixed fraction of the site radius), all such pits having the same contact angle θ and

half-angle α . A precise nucleation radius r_N can then be defined from [4]. If $r_d > r_N$, there will be no heterogeneous nucleation. If $r_d < r_N$, heterogeneous nucleation will take place in all pores with radius $r_p > [\cos(\theta - \alpha) / \beta] r_d$. However, while in most pores growth would be limited to the pit mouths (with negligible effect on volume considerations), occupancy of the entire pore elements will occur only in those with radius $r_p > (1/\beta)r_d$. With this type of simple, but instructive, model it is possible to make a quantitative assessment of nucleation, as discussed in later sections.

One concludes that the relative contribution of heterogeneous nucleation to primary desorption can be measured by the ratio of the maximum pit width to the percolation radius, $\beta r_{s,max} / r_{pt}$ or $\beta r_{s,max} / \lambda_b$, in view of [6b]. The use of the maximum site size should be noted. When this ratio is substantially less than unity, for instance in relatively narrow size distributions, we anticipate that nucleation-free percolation dominates the process. Several practical applications are likely to satisfy this condition. In the opposite case, vapor occupancy of pore elements would also occur from internal sources (nucleation sites). While the likelihood of the latter is less, a quantitative assessment of its importance would be desirable and is explored below.

(iii) Accessibility Functions

The uncertainty in the precise estimate of nucleation effects necessitates the use of a probabilistic approach. We shall postulate that at any pressure level, parametrized by r_d , a

fraction f_q of the sites (or f_p of bonds) with radius $r > r_d$ is also allowed to undergo a liquid-to-vapor transition via (heterogeneous) nucleation. The resulting vapor-liquid menisci advance and occupy adjacent pores until a pore throat with radius smaller than r_d is encountered. In the absence of a specific model, the nucleation probability fraction f_q (in general, variable with r_d or pressure) is unknown. Therefore, the accessibility functions derived below are general and apply to any functional f_q (or f_p). Note that for the simple model introduced in the previous section, the nucleation fraction (f_q or f_p) at any r_d can be simply obtained

$$f_i = \int_{r_d/\beta}^{\infty} \alpha_i(r) dr \quad [11]$$

As noted in (1) the two probabilities $q = \int_{r_d}^{\infty} \alpha_s(r) dr$, $p = \int_{r_d}^{\infty} \alpha_b(r) dr$ represent the number fraction of bonds and sites in the allowed interval $[r_d, \infty]$. For simplicity, the two fractions will be related by the previous expression (12)

$$(1-q) = (1-p)^Z \quad [12]$$

A generalization to arbitrary sizes is presented in the next Section. As previously pointed out, the analysis for secondary desorption does not include effects of local hysteresis.

It is recalled that, in the absence of nucleation, primary desorption is an ordinary percolation (1,9,12,14,15,23), while secondary desorption requires the solution to a growth problem from a fixed number of sources (1). In the presence of nucleation, the desorption process (primary or secondary) is

neither of the above. Here, in addition, sources (sites or bonds) are constantly generated during the process. As in (1), three cases are distinguished, pertaining to bond percolation (no site participation), site percolation (no bond participation), and a mixed site-bond problem. The analysis is for a Bethe lattice, although appropriate algorithms for regular lattices may be readily constructed.

a. Bond Percolation

At the initiation of secondary desorption, a fraction p_i of bonds are vapor-occupied (initial sources). At any stage $p > p_i$, the fraction of bonds allowed for vapor occupancy is p . Some allowed pores will be connected to initial sources, some will be connected to generated sources in the newly allowed interval, $p - p_i$, and some will be isolated without access to either type of sources. Denoting the actually occupied fraction by $P_b(p; p_i, f_p)$ and the isolated fraction by I_b , we obtain

$$P_b(p; p_i, f_p) = p - I_b(p; p_i, f_p) \quad [13]$$

The fraction I_b consists of isolated clusters of bonds of various sizes. A bond in any such cluster has size in $[r_d, r_i]$ (probability $p - p_i$) and may not be a source bond (probability $1 - f_p$). Furthermore, all perimeter bonds have sizes in the interval $[0, r_d]$ (probability $1 - p$). Therefore, the total isolated fraction at any stage is

$$I_b(p; p_i, f_p) = \sum_{n=1}^{\infty} B_n (p - p_i)^n (1 - f_p)^n (1 - p)^{t_n} \quad [14]$$

where B_n is the configuration coefficient (16)

$$B_n = \frac{2(Z-1)[(n+1)(Z-1)-1]!}{(n-1)! t_n!} \quad [15]$$

and t_n is the perimeter,

$$t_n = (Z-2)n + Z \quad [16]$$

The infinite series in [14] can be evaluated (16,1)

$$P_b(p; p_i, f_p) = p - (1-f_p)(p-p_i) [(1-p)/(1-x)]^{2(Z-1)} \quad [17]$$

where x is the solution in the interval $[0, 1/(Z-1)]$ of

$$x(1-x)^{Z-2} = (1-f_p)(p-p_i)(1-p)^{Z-2} \quad [18]$$

Equations [17] and [18] give the accessible fraction for bond percolation and a nonzero nucleation probability fraction f_p . The latter can vary with p as desired. The agreement with (1) in the absence of nucleation ($f_p=0$) is noted. Figures 3a and 3b depict the accessibility functions obtained for $p_i=0$ (primary desorption), and $p_i=0.05$ (secondary desorption), respectively, for $Z=4$ and various values of the constant f_p . It is apparent that, in the presence of nucleation, the sharpness of the primary desorption curve is greatly reduced as the nucleation probability increases.

b. Site Percolation

A similar approach is taken for site percolation. We shall omit the details and simply note that both the configuration coefficient and the perimeter are different than those in bond percolation (16,1). The final result is

$$P_s(q; q_i, f_q) = q - (1-f_q)(q-q_i) [(1-q)/(1-x)]^Z \quad [19]$$

where x solves [18] with q , q_i , f_q substituted in place of p , p_i , f_p , respectively. The accessibility functions are qualitatively similar to those in Fig. 3a as shown in Fig. 4.

c. Mixed Bond-Site Problem

We next examine the site accessibility in a bond-controlled

process, which is most pertinent to capillary desorption, and to many other drainage processes as well. For simplicity, it is assumed that only sites are likely to generate sources (nucleation, in pore bodies only), although the alternative is also straightforward (36). The quantity of interest is the accessible fraction of sites, given an allowed fraction of bonds.

Since the process is controlled by bonds, the fraction of isolated sites is determined by firstly evaluating the fraction of isolated bonds, and subsequently calculating the number of associated sites. The accessible fraction $X_{s,i}$ will be

$$X_{s,i} = q - I_{s,b}(p; p_i, f_q) \quad [20]$$

As before, attention is paid to $I_{s,b}$. At any stage r_d , each bond of an isolated cluster has size in $[r_d, r_i]$ (probability $p-p_i$). The condition for the bond cluster to be isolated is that all perimeter sites have size in the interval $[0, r_d]$ (probability $1-p$). Additionally, none of the sites contained in the isolated cluster may be a nucleation site. The probability of the latter event is $(1-f_q)^{n+1}$. The density of isolated clusters of size n is thus

$$P_{b,n} = B_n (p-p_i)^n (1-f_q)^{n+1} (1-p)^t \quad [21]$$

The number fraction of bond clusters of size n is simply $P_{b,n}/n$. The associated fraction of sites is obtained directly by noting that a bond cluster of size n defines a site cluster of size $n+1$, that Z bonds emanate from each site, and that each site is shared by two bonds. Then,

$$I_{s,b} = \frac{Z}{2} \sum_{n=1}^{\infty} \frac{n+1}{n} B_n (p-p_i)^n (1-f_q)^{n+1} (1-p)^t \quad [22]$$

Evaluation of the series leads to the final result

$$X_{s,i} = [1-(1-p)^Z] - (1-f_q) \{[(1-p)/(1-x)]^Z - (1-p)^Z\} \quad [23]$$

where x solves

$$x(1-x)^{Z-2} = (p-p_i)(1-f_q)(1-p)^{Z-2} \quad [24]$$

In the limit $f_q=0$, we obtain previously developed expressions for secondary desorption in the absence of nucleation (1). Figures 5a and 5b show the results obtained for $Z=4$, various values of f_q (taken constant), $p_i=0$ and $p_i=0.05$, respectively. As with Figure 3, a notable effect due to nucleation is observed.

3. ARBITRARY SIZE DISTRIBUTIONS

The previous expressions for the mixed problem were based on the assumption that site and bond distributions are related by [12]. Figure 6 shows a schematic of this constraint for a fixed bond size distribution. An increase in Z leads to a corresponding shift of the site distribution towards larger sizes. This interesting effect is worth noting since it couples geometry and topology in the porous medium. The underlying principle is that no pore body has size smaller than its associated Z pore throats. However, as noted previously, expression [12] is only the marginal limit of the stronger statement (14)

$$q \geq 1 - (1-p)^Z \quad [25a]$$

for every q and p . In fact, it may be shown (36) that the additional constraint

$$q \geq p^{\frac{1}{2}} \quad [25b]$$

derived from the condition that a bond has size smaller than the adjacent two sites, must also be satisfied (see also (38)).

Equivalently,

$$\int_0^r \alpha_s(r') dr' \leq \min \left\{ \left[\int_0^r \alpha_b(r') dr' \right]^2, 1 - \left(\int_r^\infty \alpha_b(r) dr \right)^2 \right\} \quad [26]$$

for every r . For any distributions, the equality sign must be obeyed at the limits $q=p=0$ ($r=\infty$) and $q=p=1$ ($r=0$). Obviously, a large variety of such functions (e.g. overlapping, non-overlapping) satisfy the above restrictions. Generalizing the previous results to arbitrary sizes as dictated by [25] is not as trivial as it might appear. In fact, it is shown below that the limiting relationship [12] plays a rather special role in a network model and facilitates calculations considerably.

(i) Associated Fraction q^*

To proceed, the associated fraction q^* will first be defined. Consider a fraction of bonds p and sites q , with the same radius

$$p = \int_r^\infty \alpha_b(r') dr', \quad q = \int_r^\infty \alpha_s(r') dr' \quad [27]$$

and assume that all such elements are actually allowed (they are occupied by vapor as in primary adsorption). By definition, all bonds are associated (terminate) with sites of size greater than r . The number fraction of these sites, q^* , will be termed the associated fraction. It will be shown that $q > q^*$, regardless of the particular size distributions,

$$q > q^* = 1 - (1-p)^2 \quad [28]$$

which is expression [12]. The proof is straightforward:

The probability that a randomly picked site is associated with at least one bond in $[r_d, \infty]$ (probability p) is equal to one minus the probability that all of the bonds emanating from it are in $[0, r_d]$ (each having probability $1-p$). The probability of the

latter event is $(1-p)^Z$, and Equation [28] follows immediately. The latter holds both below and above the percolation threshold, p_c , and yields the total fraction of sites associated with either finite or infinite bond clusters.

To obtain the fraction contained in finite clusters requires some analysis. Bond clusters of size n have the usual probability

$$P_n = B_n p^n (1-p)^{t_n} \quad [29]$$

while their number is P_n/n . Applying the usual reasoning that Z bonds emanate from each site, each bond is shared by two sites, and $(n+1)$ sites associate with a bond cluster of size n , the total fraction of sites associated with finite bond clusters is

$$\begin{aligned} q_F^* &= \frac{Z}{2} \sum_{n=1}^{\infty} (n+1) [P_n/n] \\ &= \frac{Z}{2} \sum_{n=1}^{\infty} \frac{n+1}{n} B_n p^n (1-p)^{(Z-2)n+Z} \end{aligned} \quad [30]$$

The latter becomes

$$q_F^* = [(1-p)/(1-x)]^Z - (1-p)^Z \quad [31]$$

where x is the solution of

$$x(1-x)^{Z-2} = p(1-p)^{Z-2} \quad [32]$$

For $p < p_c = 1/(Z-1)$, the relevant root is $x = p$. Substitution in [31] yields [28] again. On the other hand, for $p > p_c$, [31] yields only the fraction associated with finite bond clusters. The fraction contained in the infinite bond cluster, q_{∞}^* , is obtained by deducting [31] from [28]

$$q_{\infty}^* = 1 - (x/p)^{Z/(Z-2)} \quad [33]$$

where x solves [32].

(ii) Absence of Nucleation

We are now in a position to proceed with the general problem. We shall first consider secondary desorption in the absence of nucleation, thereby extending the percolation problem in (1) to arbitrary size distributions. The mixed bond-site problem is examined.

At the conclusion of adsorption ($r=r_i$), a set of bonds and sites of fraction p_i and q_i , respectively, are vapor-occupied. Given p_i , the associated fraction of sites q_i^* is defined. The remainder set ($q_i - q_i^*$) is occupied by vapor but it is associated (connected) with bonds that have size smaller than r_i . At any stage $r_d < r_i$ during secondary desorption, this fraction ($q_i - q_i^*$) may further be viewed as connected to bonds in either $[r_d, r_i]$ (probability $p - p_i$) or in $[0, r_d]$ (probability $1 - p$).

Consider now an isolated bond cluster. It contains interior bonds in $[r_d, r_i]$ (probability $p - p_i$), perimeter bonds in $[0, r_d]$ (probability $1 - p$), and includes sites that may not be initial source sites. The probability for a site to satisfy the latter condition is $(1 - q_i) / (1 - q_i^*)$, if one notes that all sites in q_i^* are contained in clusters that have bonds in $[r_i, \infty]$ (probability p_i), thus, they cannot be associated with bonds of smaller size. The fraction of sites associated with such bond clusters is calculated as before. We obtain the isolated fraction

$$I_{s,b} = \frac{Z}{2} \sum_{n=1}^{\infty} \frac{n+1}{n} B_n (p - p_i)^n (1 - p)^t \left[\frac{(1 - q_i)}{(1 - q_i^*)} \right]^{n+1} \quad [34]$$

which, after evaluation of the series becomes

$$I_{s,b} = \{[(1-p)/(1-x)]^Z - (1-p)^Z\} (1-q_i)/(1-q_i^*) \quad [35]$$

where x is the solution of the equation

$$x(1-x)^{Z-2} = (p-p_i)(1-p)^{Z-2}(1-q_i)/(1-q_i^*) \quad [36]$$

The accessible fraction of sites at any stage p can be now evaluated. It shall consist of three terms

$$X_{s,i} = q^* - I_{s,b} + S_i \quad [37]$$

The presence of q^* instead of q on the first term reflects the fact that in this bond percolation process, only sites associated with allowed bonds (of fraction p) are eligible (contrast with [20]). The second term is the usual isolated fraction. Finally, S_i denotes the fraction of initial vapor sites, which are surrounded by bonds of size in $[0, r_d]$ (probability $1-p$)

$$S_i = [(q_i - q_i^*)/(1 - q_i^*)](1-p)^Z \quad [38]$$

This latter set contains vapor-occupied sites not included in q^* , and must be accounted for. Upon substitution of [28], [35], and [38] in [37], the simple expression is obtained

$$X_{s,i} = 1 - [(1-q_i)/(1-q_i^*)] [(1-p)/(1-x)]^Z \quad [39]$$

where x solves [36]. It is interesting to note that, in contrast to the nucleation case below, the accessibility functions are independent of the current value of the site fraction q , although they do depend on the initial value q_i . In the absence of nucleation, the only way a liquid-occupied site changes occupancy is by becoming connected to a source site via allowed bonds. This mechanism is independent of the site distribution function.

We test three limiting cases. First, $X_{s,i}=1$ in the limit $q_i=1$, as expected. Second, if $q_i=q_i^*$ (all source sites associated with source bonds), [39] and [36] reduce to the expressions derived previously (1). Finally, when $q_i=0$, we obtain the

ordinary percolation results in (12), (1), since q_1^* and p_i are necessarily equal to zero. Figures 7a and 7b show the resulting accessibility functions for the two values $p_i=0$ and $p_i=0.05$, for various values of q_i and for $Z=4$. The notable departure from the previous cases (1) should be noted.

(iii) Nucleation Effects

The above can be easily extended to include nucleation effects. For simplicity, only nucleation in sites (pore bodies) will be considered. At any stage r_d , a fraction (in general variable) f_q of the sites with radius $r > r_d$ can be activated to generate internal sources for vapor occupancy of adjacent sites and bonds. The method of evaluating accessibility is as follows.

We distinguish four sets of sites. One contains all sites associated with bonds in $[r_d, \infty]$, of fraction q^* . The second set is the usual isolated fraction, with the additional requirement that sites may neither be initial sources (probability per site $(1-q_1)/(1-q_1^*)$), nor nucleation sites (probability $1-f_q$). The isolated fraction becomes

$$I_{s,b} = \frac{Z}{2} \sum_{n=1}^{\infty} \frac{B_n (p-p_i)^n (1-p)^t}{n} (1-f_q)^{n+1} [(1-q_1)/(1-q_1^*)]^{n+1} \quad [40]$$

which is evaluated to yield

$$I_{s,b} = (1-f_q) \{ [(1-p)/(1-x)]^Z - (1-p)^Z \} (1-q_1)/(1-q_1^*) \quad [41]$$

The third set comprises sites that are initially occupied by vapor and completely surrounded by liquid-occupied bonds in $[0, r_d]$ (probability $1-p$). The final set contains all sites that are in $[r_d, \infty]$, but not associated with bonds in $[r_d, \infty]$, they are initially not occupied by vapor (probability $(1-q_1)/(1-q_1^*)$), and

they become nucleation sites (probability $(q-q^*)f_q$). The accessible fraction is, thus,

$$X_{s,i} = \{1-(1-p)^Z\} - \{(1-f_q)\{[(1-p)/(1-x)]^Z (1-q_i)/(1-q_i^*) - (1-p)^Z\}\} \\ + \{(1-p)^Z(1-q_i)/(1-q_i^*)\} + \{(q-q^*)f_q(1-q_i)/(1-q_i^*)\} \quad [42]$$

where x is the solution of

$$x(1-x)^{Z-2} = (p-p_i)(1-p)^{Z-2}(1-f_q)(1-q_i)/(1-q_i^*) \quad [43]$$

Note that, unlike the previous case, the site accessibility here also depends on the current value of q . One interesting limit is $p=0$ in the case $q_i=p_i=0$. Then, $X_{s,i} = qf_q$, as expected, since only the sites that can nucleate are occupied by vapor. Also in agreement, the percolation limit considered in (1), (12) is obtained, when $q_i=p_i=0$ and $f_q=0$.

4. DISCUSSION

An illustration of some of the above effects will be next presented. Figure 8 depicts calculated primary desorption curves for nitrogen at 78°K. A Bethe lattice representation was used, with a coordination number $Z=4$. Both bond and site sizes were assigned a Rayleigh distribution

$$\alpha_b(r) = \frac{\pi}{2} \frac{(r-r_0)}{(r_a-r_0)^2} \exp\left\{-\frac{\pi}{4} \frac{(r-r_0)^2}{(r_a-r_0)^2}\right\} \quad [44]$$

with minimum and average values, $r_0=10$ Angstrom and $r_a=20$ Angstrom for bonds, and $r_0=15$ and $r_a=45$ for sites, respectively. Liquid saturations were evaluated using (42) along with the assumptions that only sites contribute to volume and the number fraction is also the volume fraction. The nucleation fraction f_q was held constant in one run (Figure 8a), and allowed to increase

during the progress of desorption in the other (Figure 8b), according to the ad hoc expression, $f_q = \exp(-aP_v/P_{v0})$. To a different degree, both cases reflect the increasing likelihood of heterogeneous nucleation as the relative pressure decreases. We note no discernible differences in the results of these two different models. Both Figures show that the desorption isotherm may rapidly lose its percolation character, provided that sufficient nucleation is allowed. The deviation resembles vapor compressibility (20) or finite size (9) effects. Similar effects exist in secondary desorption.

In the above, the nucleation fraction was left largely arbitrary. In reality, this is in general not the case, as pointed out by the simple model of Section 2. To illustrate the difference, nucleation effects corresponding to [11] are shown in Figure 9, with all other parameters held constant. It is recalled that the parameter β is the ratio of pit size to pore size, in general a small number (e.g., 0.1-0.3). For the latter range, it is suggested from the results of Figure 9, that nucleation effects in capillary desorption may not be overemphasized. Equivalently, if either one of the previous ad hoc models were to be used, constant fractions f_q should be not greater than 0.05, while parameter "a" should be not smaller than 5. Of course, the self-similarity and uniformity assumed in [11] are not expected to hold in general, although the former is often a property of fractal structures. A more accurate model may perhaps be constructed with the parameter β being a distributed variable, to reflect wettability non-uniformity, and the additional increase in the fraction of activated nucleation sites upon a pressure

decrease.

As stressed previously, homogeneous nucleation should be negligible in properly designed desorption experiments, while effects of heterogeneous nucleation may be present, since the latter is size-specific. As stressed above, and for typical cases, this likelihood (f_q) is expected to be small in the range of relative pressures near the onset of desorption. At the same time, it should be kept in mind that, in porous media with long tails in the size distributions and with sufficient heterogeneity in wettability properties, heterogeneous nucleation effects can become comparable to percolation. Such may be the case in phase change processes in natural porous rocks (e.g. geothermal reservoirs).

The effect of arbitrary size distributions on secondary desorption is shown in Figure 10. To illustrate a notable feature, distributions with a maximum cut-off size in nucleation-free ($f_q=0$) processes were considered. We take Rayleigh-type statistics with $r_0=10$, $r_a=15$, and $r_{b,max}=25$ Angstrom for bonds, and 15, 25, and 45 Angstrom for sites, respectively. All other parameters take the same values as in Fig. 8. We note that some of the secondary isotherms are flat for a range of relative pressures after the initiation of desorption, since no phase change would occur until the pressure is reduced to that corresponding to the largest pore throat. This feature is inherently absent in media satisfying [12] and it could be used to identify the largest throat size, provided of course that other effects (resolution, nucleation, compressibility, etc.)

would not obscure the interpretation of the data.

It should be emphasized that in a network model, bonds and sites can be assigned sizes at random provided that relation [26] is not violated. We recall, that the first of the restrictions follows by noting that the fraction of sites in an interval (r_d, ∞) is, in general, greater than the fraction associated with bonds in the same size interval. Similarly, the second restriction expresses the fact that the fraction of bonds in the size interval $(0, r_d)$ is generally greater than the fraction associated with sites in the same size interval (36). When local hysteresis in bonds during the two processes (adsorption/desorption) is neglected, relationship [25b] does not enter in any of the accessibility calculations although, of course, the distributions must still satisfy the restriction. Incorporating the local hysteresis into a network model does not appear to be as trivial as one might expect, even when the volumetric contribution of bonds is neglected. While primary processes and secondary adsorption remain unaffected by local hysteresis, secondary desorption would be altered. Additionally, if the bond volume is not ignored, all processes would be influenced. The significance of this effect is currently being investigated.

In our previous work (1), the following relationship between the slopes of secondary desorption and primary adsorption at the onset of desorption

$$ds_{L,SD}/ds_{L,A} = 1 - (1-p_i)^{Z-1} \quad [45a]$$

was suggested as a means for the direct estimation of the throat density function $\alpha_b(r)$, subject to [12]. The extension of [45a]

to the more realistic case [25] can be readily obtained

$$dS_{L,SD}/dS_{L,A} = Z \frac{d(1-p_i)}{d(1-q_i)} \left[\frac{(1-q_i)}{(1-p_i)} - \frac{(1-q_i)^2}{(1-p_i)^2} \right] \quad [45b]$$

In contrast to [45a], however, now it is a differential rather than an algebraic equation that relates data (LHS) to parameters (RHS). When [12] is assumed, [45a] can be used to estimate p_i , and the adsorption data would yield the volume distribution $V_S(r)$. In the general case [28], on the other hand, an assumption about the volume distribution $V_S(r)$ is necessary, for further progress. The adsorption data may then yield q_i (hence, $\alpha_S(r)$), which is to be used for a (numerical) integration of [45b]. Figure 11 portrays a typical schematic of secondary desorption isotherms for some model distribution satisfying [25a]. It can be reasonably argued that an assumption about the volume of a site is more justifiable than the postulate [12]. For both cases, of course, the coordination number Z must be properly chosen to match the percolation threshold. This may require a trial-and-error procedure. It should be also cautioned, that relations [45] have been derived based on a Bethe lattice representation, and may not warrant application to other networks.

A limitation of the above analysis is the thermodynamic equilibrium assumed in the occupancy of pore elements, although one should also note the kinetic considerations in estimating nucleation effects. Equilibrium times associated with capillarity in porous media vary with the size distributions, among other variables, long times associated with systems with disparate scales (26). Under this qualification, the above may be extended

to other growth processes perhaps with some modifications.

Nucleation in multicomponent systems in porous media (e.g. oil-gas mixtures) are interesting processes, where diffusion may introduce additional non-local effects. Application of the more general relationship [25] to immiscible phase equilibria and flow (capillary pressure, phase permeabilities (31, 32)) would affect currently used models for quasistatic flow in porous media. Extensions to other related processes following the lines of (25) are obvious directions. Finally, the investigation of such processes in regular lattices may be worth considering.

5. SUMMARY

The present study is an extension of previous work in capillary sorption processes in porous media. The issues of nucleation and pore size distributions were explored in more detail. It was concluded that homogeneous nucleation may be negligible in typical vapor desorption experiments. Heterogeneous nucleation, being pore size-specific, has a higher likelihood to affect the desorption isotherms. Simple models were developed to account for the latter case in Bethe lattice pore networks.

Deviations from a percolation behavior, previously attributed to compressibility (20) and finite size (9), can likewise be explained by nucleation.

Consideration of largely arbitrary pore size distributions leads to a non-trivial modification of the previous expressions.

While primary desorption is unaffected, secondary processes are notably influenced, particularly in the presence of nucleation.

It is suggested that such effects are inherently present to any

network model of porous media, and should be accounted for in the various capillary processes, where site occupancy and volumetric estimates are dictated from bond connectivity.

ACKNOWLEDGEMENT

This study was partly supported by DOE Contract DE-FG19-87BC14126, the contribution of which is gratefully acknowledged.

1. Gredg, S.J., Colloids and Surfaces, **11**, 109 (1983).
2. Adamson, A.W., "Physics of Solid Surfaces", Wiley, New York, 1962.
3. Gredg, S.J. and Sing, K.S.W., "Adsorption, Surface Area and Pore Volume", Academic Press, New York, 1982.
4. Everett, D.H., "The Solid-Gas Interface." (E.A. Flood, Ed.), Dekker, New York, 1967.
5. Everett, D.H. and Haynes, J.M., J. Colloid Interface Sci., **38**, 122 (1972).
6. Everett, D.H., J. Colloid Interface Sci., **52**, 109 (1975).
7. Fatt, I., Trans. AIME, **207**, 144 (1956).
8. Wall, G.C. and Brown, R.S.C., J. Colloid Interface Sci., **82**, 141 (1981).
9. Broadbent, S.R. and Hammersley, J.M., Proc. Cambridge Philos. Soc., **53**, 629 (1957).
10. Stauffer, D., "Introduction to Percolation Theory", Taylor & Francis, Philadelphia, 1985.
11. Mason, G., Proc. R. Soc. London A320, **47** (1983).
12. Mason, G., J. Colloid Interface Sci., **92**, 277 (1983).
13. Mason, G., Proc. R. Soc. London A112, **453** (1980).
14. Nelmark, A.V., Colloid J., **46**, 613 (1984).
15. Fisher, M.E. and Essam, J.W., J. Math. Phys., **2**, 609 (1961).
16. Flory, P.J., "Principles of Polymer Chemistry", Cornell Univ. Press, New York, 1953.
17. Brown, S.J., Ph.D. Dissertation, University of Bristol, 1983.
18. Emmett, P.H. and Cline, M., J. Phys. Chem., **51**, 1248 (1947).
19. Schachter, R.S., Wade, W.H., and Wingrave, J.A., J. Colloid Interface Sci., **59**, 7 (1977).
20. Haynes, J.M. and McCaffery, F.G., J. Colloid Interface Sci., **59**, 24 (1977).

REFERENCES

1. Parlar, M. and Yortsos, Y.C., J. Colloid Interface Sci. 124, 162 (1988).
2. Gregg, S.J., Colloids and Surfaces 21, 109 (1986).
3. Adamson, A.W., "Physical Chemistry of Surfaces." Wiley, New York, 1982.
4. Gregg, S.J. and Sing, K.S.W., "Adsorption, Surface Area and Porosity." Academic Press, New York, 1982.
5. Everett, D.H., "The Solid-Gas Interface." (E.A. Flood, Ed.), Dekker, New York, 1967.
6. Everett, D.H. and Haynes, J.M., J. Colloid Interface Sci. 38, 125 (1972).
7. Everett, D.H., J. Colloid Interface Sci. 52, 189 (1975).
8. Fatt, I., Trans. AIME 207, 144 (1956).
9. Wall, G.C. and Brown, R.J.C., J. Colloid Interface Sci. 82, 141 (1981).
10. Broadbent, S.R. and Hammersley, J.M., Proc. Cambridge Philos. Soc. 53, 629 (1957).
11. Stauffer, D., "Introduction to Percolation Theory." Taylor & Francis, Philadelphia, 1985.
12. Mason, G., Proc. R. Soc. London A390, 47 (1983).
13. Mason, G., J. Colloid Interface Sci. 95, 277 (1983).
14. Mason, G., Proc. R. Soc. London A415, 453 (1988).
15. Neimark, A.V., Colloid J. 46, 813 (1984).
16. Fisher, M.E. and Essam, J.W., J. Math. Phys. 2, 609 (1961).
17. Flory, P.J., "Principles of Polymer Chemistry." Cornell Univ. Press, New York, 1953.
18. Brown, A.J., Ph.D. Dissertation, University of Bristol, 1963.
19. Emmett, P.H. and Cines, M., J. Phys. Chem. 51, 1248 (1947).
20. Schechter, R.S., Wade, W.H., and Wingrave, J.A., J. Colloid Interface Sci. 59, 7 (1977).
21. Haynes, J.M. and McCaffery, F.G., J. Colloid Interface Sci. 59, 24 (1977).

22. Barrett, E.P., Joyner, L.G., and Halenda, P.P., J. Amer. Chem. Soc. 73, 373 (1951).
23. Zhdanov, V.P., Fenelonov, V.B., and Efremov, D.K., J. Colloid Interface Sci. 120, 218 (1987).
24. Morrow, N.R., Ind. Eng. Chem. Fund. 62, 32 (1970).
25. Parlar, M. and Yortsos, Y.C., Paper SPE 16969, presented at the 62nd Annual Meeting of SPE-AIME, Dallas, TX, Sept. 27-30, 1987.
26. Thompson, A.H., Katz, A.J., and Krohn, C.E., Adv. in Phys. 36, 625 (1987).
27. Avnir, D., Farin, D., and Pfeifer, P., J. Colloid Interface Sci. 103, 112 (1985).
28. Brunauer, S., Emmett, P.H., and Teller, E., J. Amer. Chem. Soc. 60, 309 (1938).
29. de Boer, J.H., Lippens, B.C., Linsen, B.G., Broekhoff, J.C.P., van den Heuvel, A., and Osinga, J., J. Colloid Interface Sci. 21, 405 (1966).
30. Dubinin, M.M., J. Colloid Interface Sci. 77, 84 (1980).
31. Heiba, A.A., Sahimi, M., Scriven, L.E., and Davis, H.T., Paper SPE 11015, presented at the 57th Annual Meeting of SPE-AIME, New Orleans, LA, Sept. 26-29, 1982.
32. Heiba, A.A., Davis, H.T., and Scriven, L.E., Paper SPE 12172, presented at the 58th Annual Meeting of SPE-AIME, San Francisco, CA, Oct. 5-8, 1983.
33. Zettlemoyer, A.C., "Nucleation." Dekker, New York, 1969.
34. Fisher, J.C., J. Appl. Phys. 19, 1062 (1948).
35. Ward, C.A., Johnson, W.R., Venter, R.D., Ho, S., Forest, T.W., and Fraser, W.D., J. App. Phys. 54, 1833 (1983).
36. Parlar, M., Ph.D. Thesis, University of Southern California (1989).
37. Forest, T.W., J. App. Phys. 53, 6191 (1982).
38. Chatzis, I., and Dullien, F.A.L., Int. Chem. Eng. 25, 47 (1985).

32. Barrett, R.P., Joyner, L.G., and Halenda, P.P., J. Amer. Chem. Soc. 73, 373 (1951).

33. Zhdanov, V.P., Penelov, V.B., and Biremov, D.K., J. Colloid Interface Sci. 120, 210 (1987).

34. Moroz, M.R., Ind. Eng. Chem. Fund. 62, 32 (1970).

35. Parlar, M. and Yortsov, Y.C., Paper SPE 16989, presented at the 62nd Annual Meeting of SPE-AIME, Dallas, TX, Sept. 27-30, 1987.

36. Thompson, A.H., Katz, A.J., and Krohn, C.E., Adv. in Phys. 36, 675 (1987).

37. Avnir, D., Farin, D., and Pefker, P., J. Colloid Interface Sci. 103, 112 (1985).

38. Brunner, S., Emmett, P.H., and Teller, E., J. Amer. Chem. Soc. 60, 309 (1938).

39. de Boer, J.H., Lippens, B.C., Linssen, B.G., Broekhoff, J.C.P., van den Hulst, A., and Ostinga, J., J. Colloid Interface Sci. 57, 405 (1966).

40. Duplain, M.M., J. Colloid Interface Sci. 77, 84 (1980).

41. Heida, A.A., Sahimi, M., Scriver, L.A., and Davis, H.T., Paper SPE 11015, presented at the 57th Annual Meeting of SPE-AIME, New Orleans, LA, Sept. 28-29, 1982.

42. Heida, A.A., Davis, H.T., and Scriver, L.A., Paper SPE 12173, presented at the 58th Annual Meeting of SPE-AIME, San Francisco, CA, Oct. 2-8, 1983.

43. Zettlemoyer, A.C., Reaction, Baker, New York, 1959.

44. Fisher, J.C., J. Appl. Phys. 1, 1062 (1940).

45. Ward, C.A., Johnson, W.R., Venter, R.D., Ho, S., Forest, T.W., and Fraxer, W.D., J. Appl. Phys. 54, 1833 (1983).

46. Parlar, M., Ph.D. Thesis, University of Southern California (1989).

47. Forest, T.W., J. Appl. Phys. 53, 6191 (1982).

48. Chakraborty, S., and Dullien, F.A.L., Ind. Chem. Eng. 25, 47 (1982).

Figure 1. Schematic of a Nucleation Site in a Pore Body.

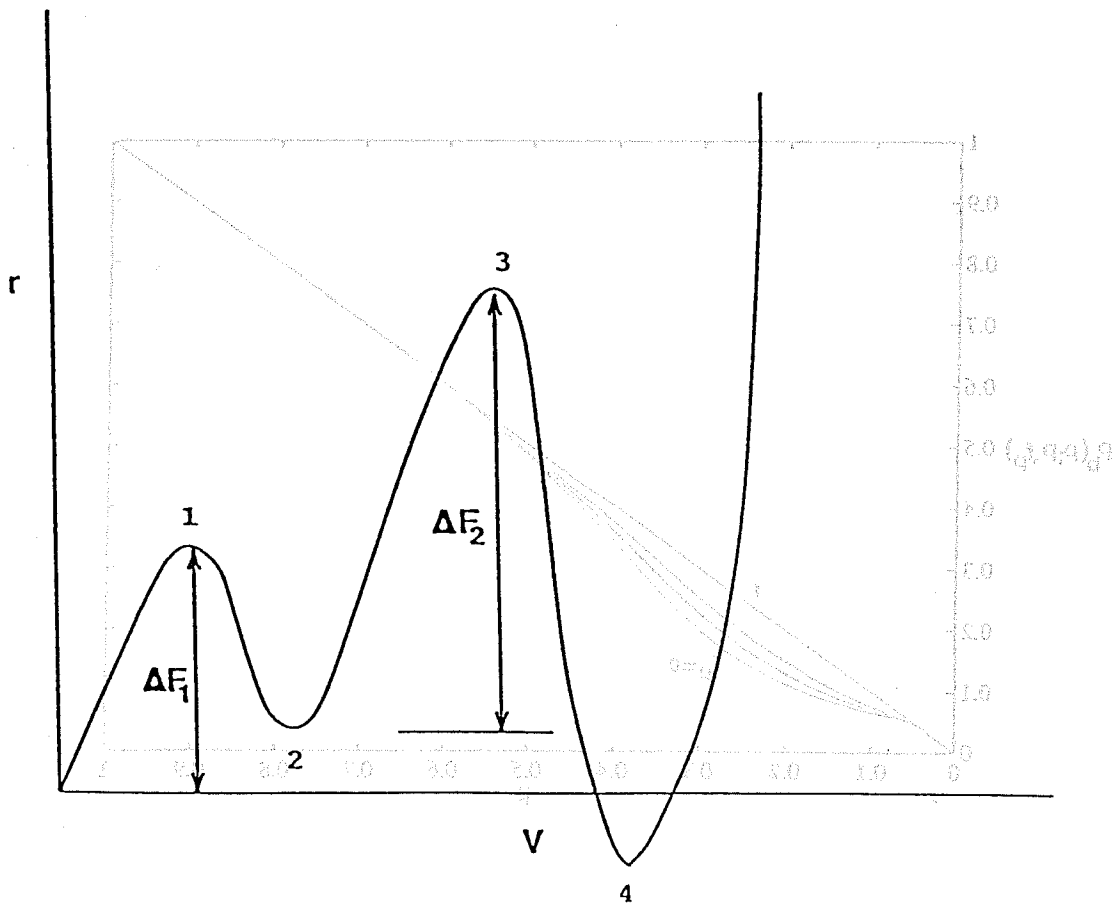
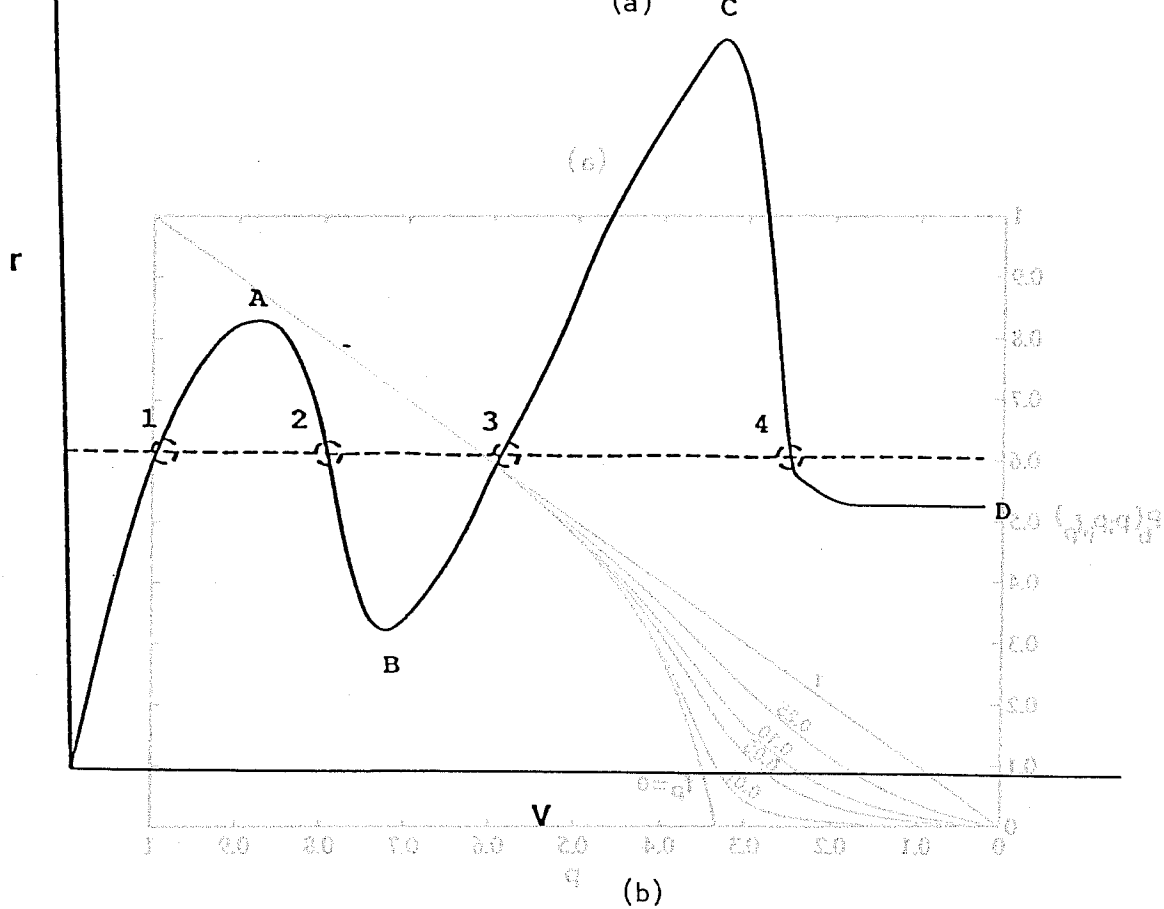


Figure 2. Nucleation in a "Hydrophobic Site". (a) Schematic of Curvature-Volume Relationship, (b) Schematic of Change in Free Energy-Volume Relationship.

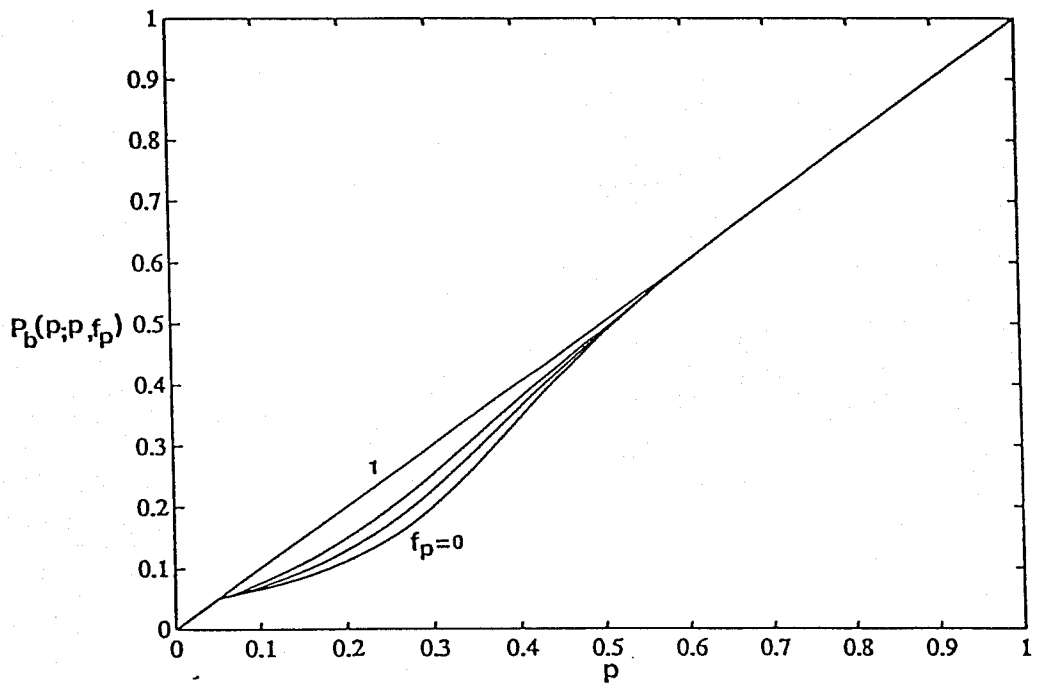
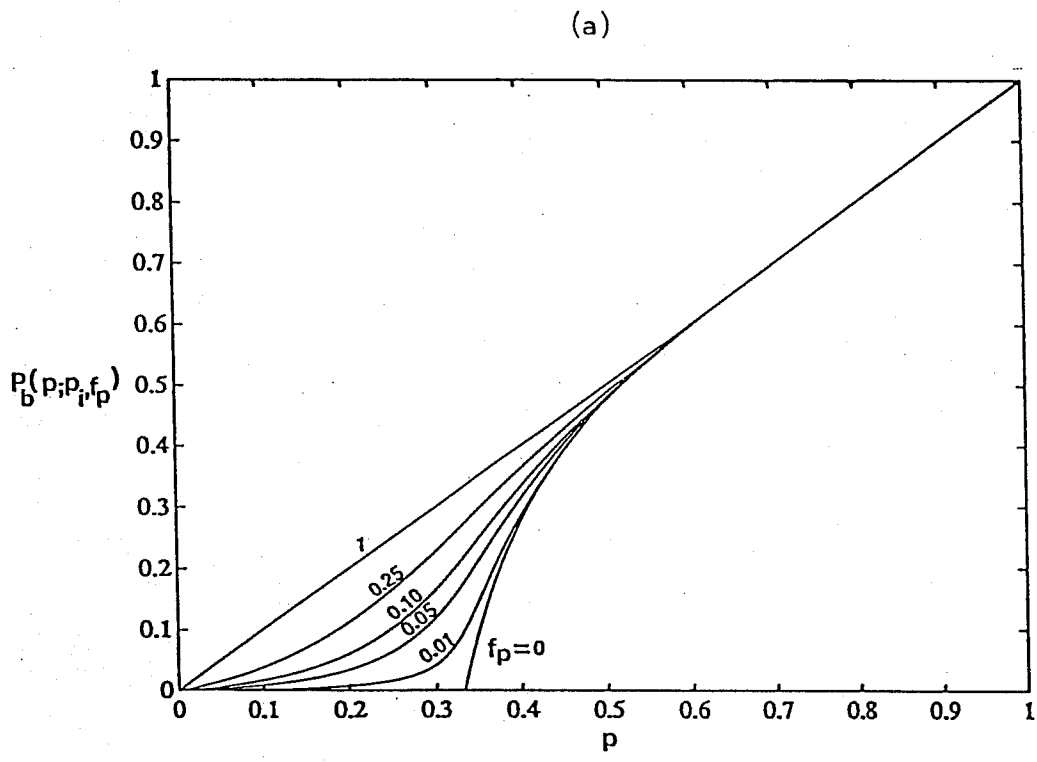


Figure 3. Accessible Fraction of Bonds as a Function of Allowed Fraction p for Various Values of f_p : $Z=4$. (a) $p_i=0$, (b) $p_i=0.05$.

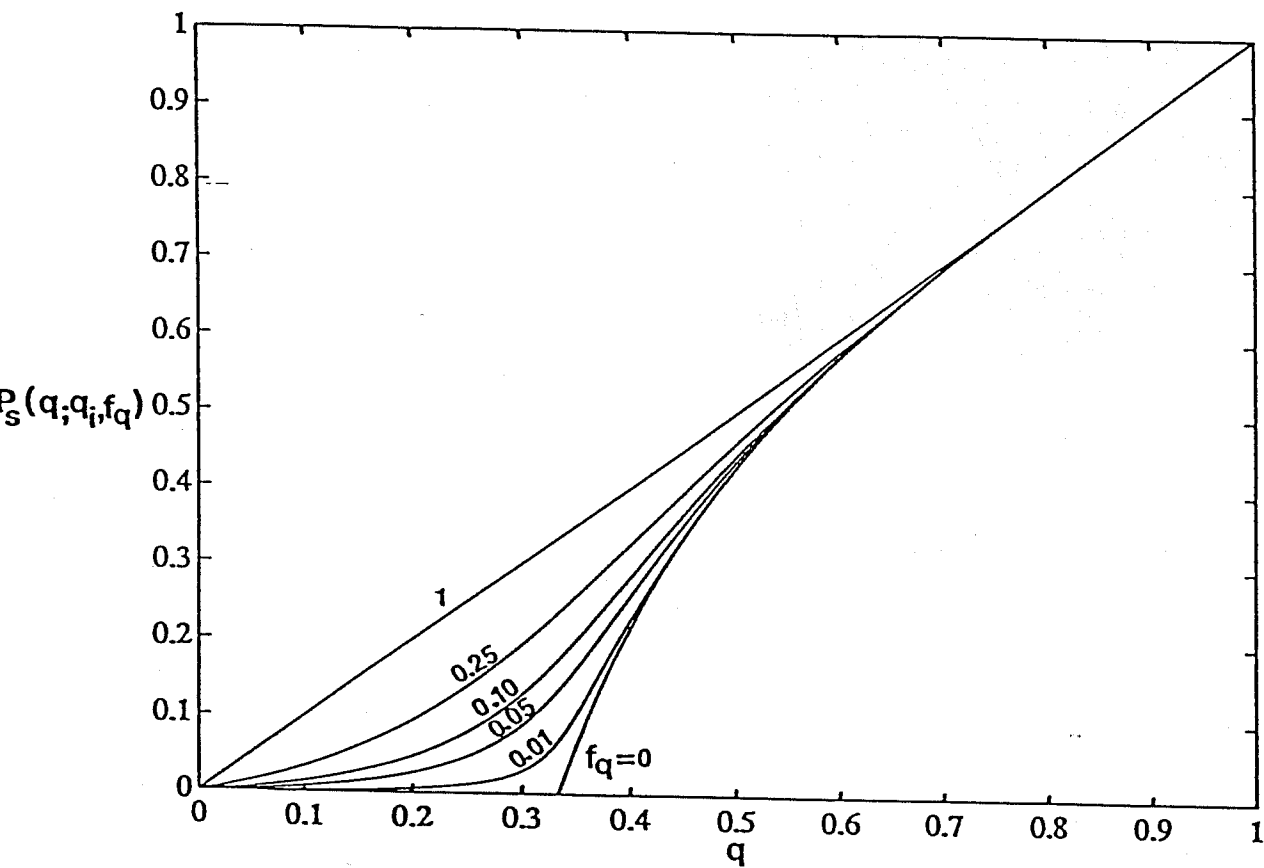


Figure 4. Accessible Fraction of Sites as a Function of Allowed Fraction q for Various Values of f_q : $Z=4$, $q_1=0$.

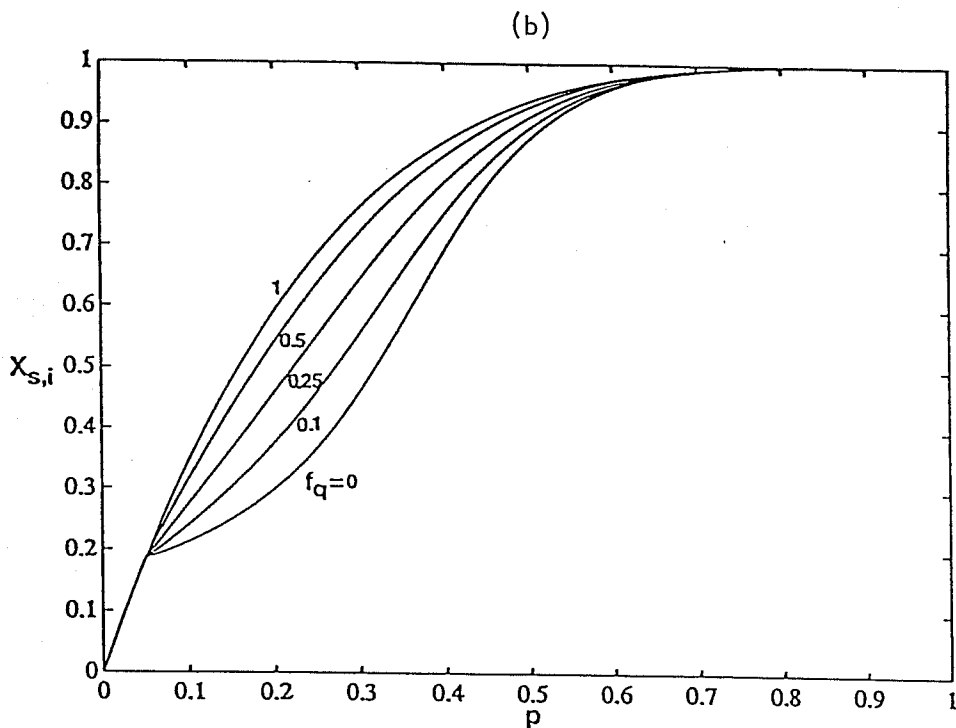
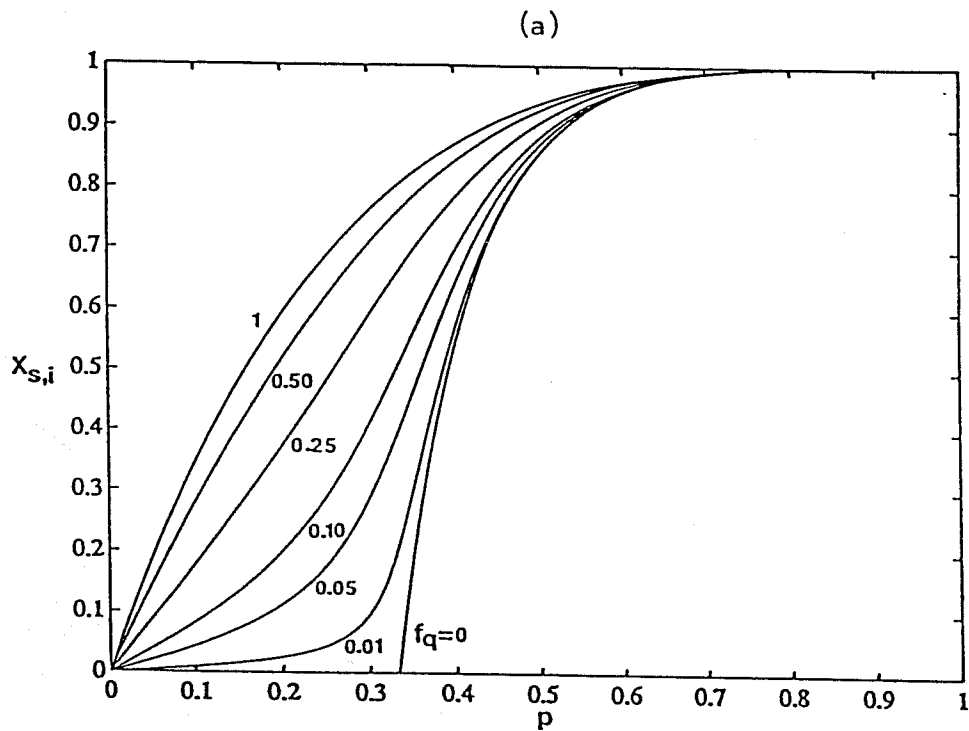


Figure 5. Accessible Fraction of Sites as a Function of Allowed Fraction p for Various Values of f_q : $Z=4$. (a) $p_i=0$, (b) $p_i=0.05$.

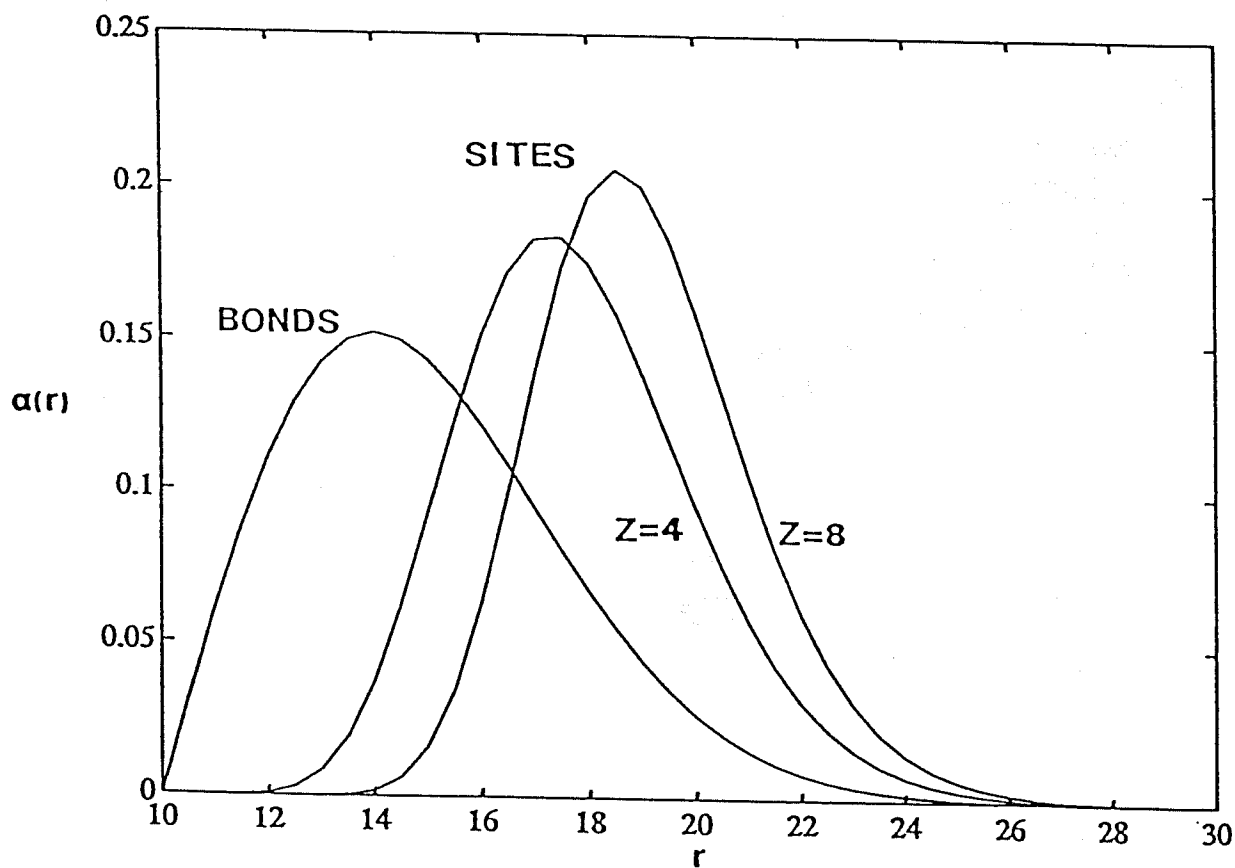


Figure 6. Effect of Coordination Number on Limiting Site Size Distribution.

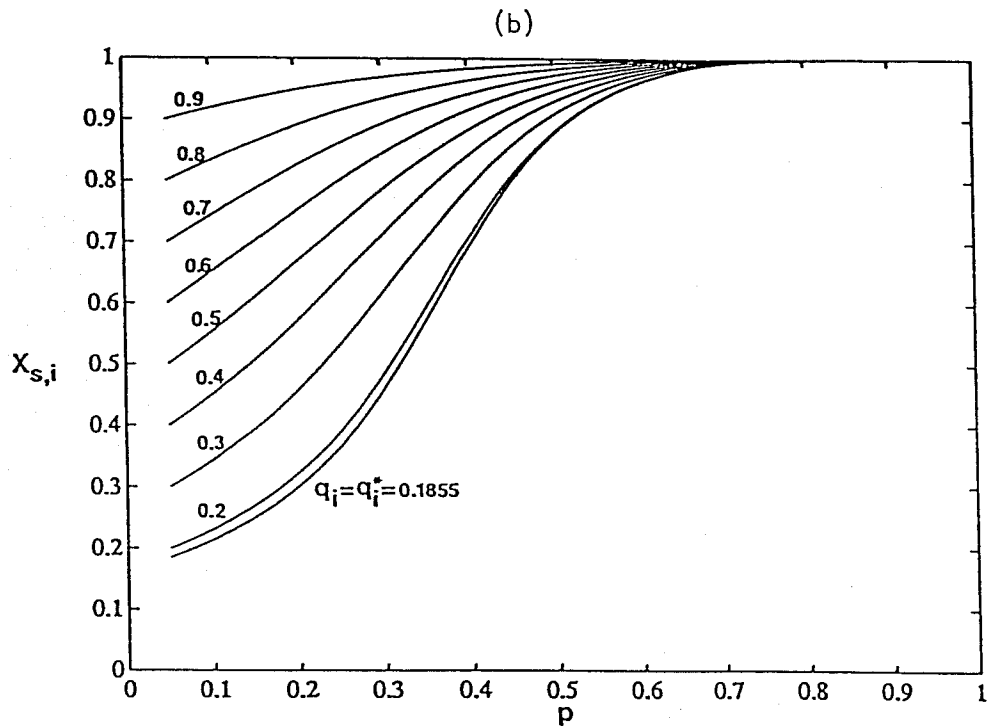
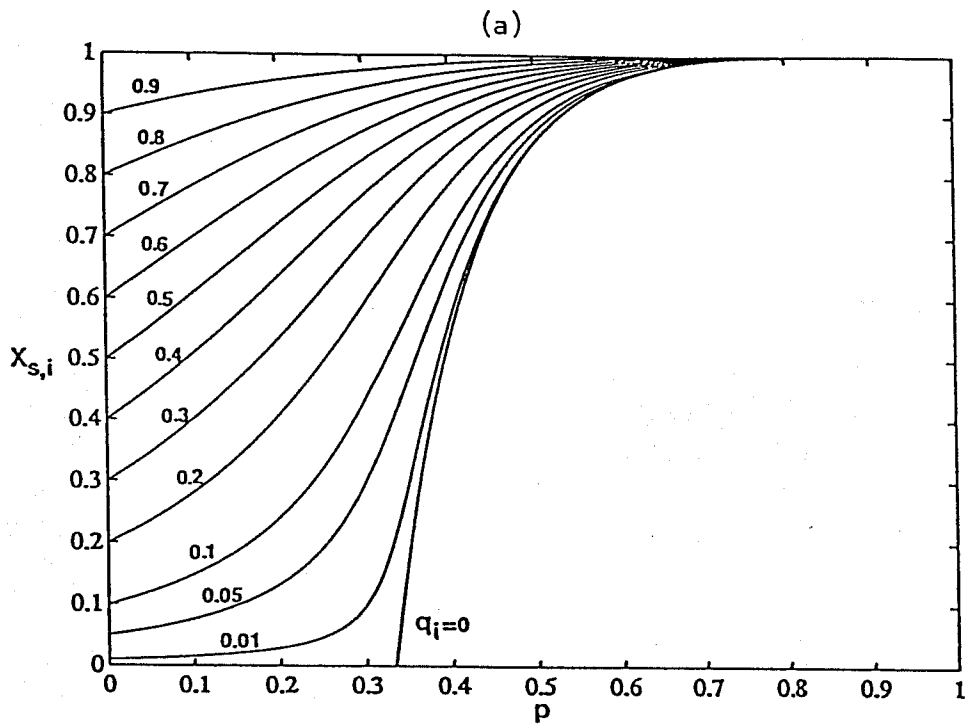


Figure 7. Accessible Fraction of Sites as a Function of Allowed Fraction p for Various Values of q_i : Arbitrary Size Distributions, $Z=4$, $f_q=0$. (a) $p_i=0$, (b) $p_i=0.05$.

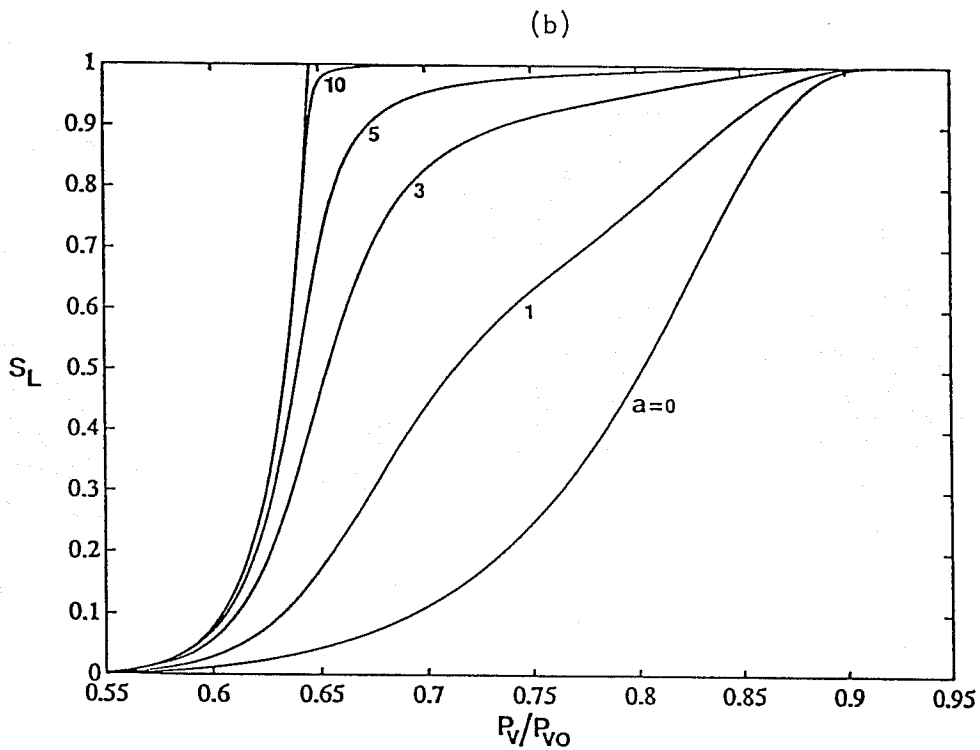
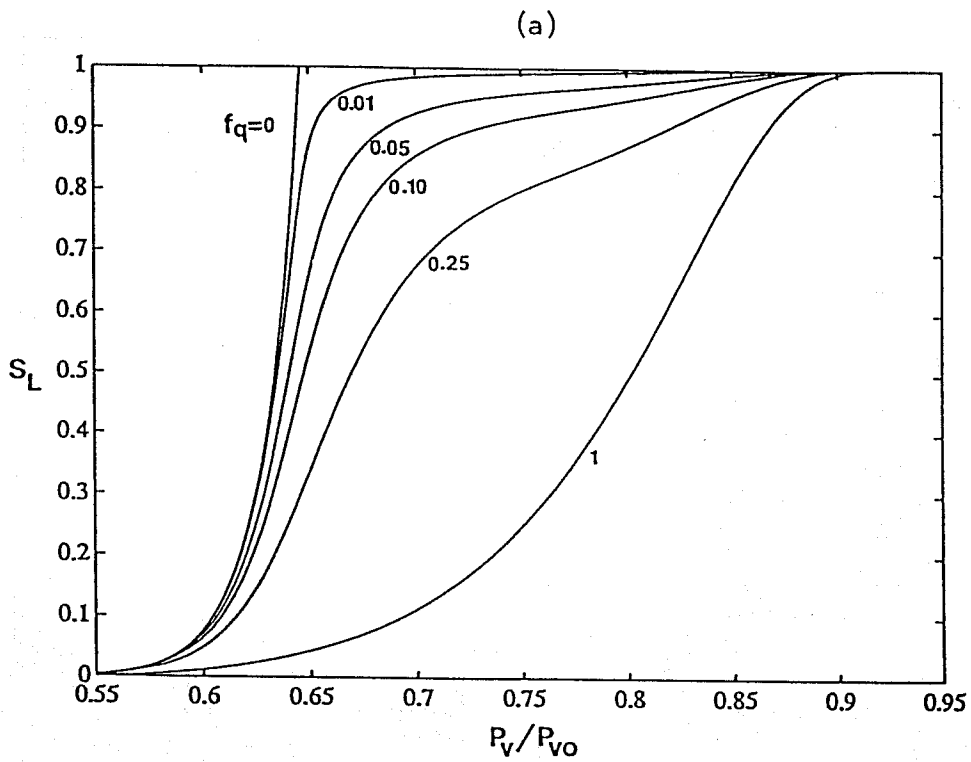


Figure 8. Model Prediction of Primary Desorption Curves for Sorption of Nitrogen for Various Values of f_q : $Z=4$.
 (a) $f_q = \text{Constant}$, (b). $f_q = \exp(-aP_V/P_{V0})$.

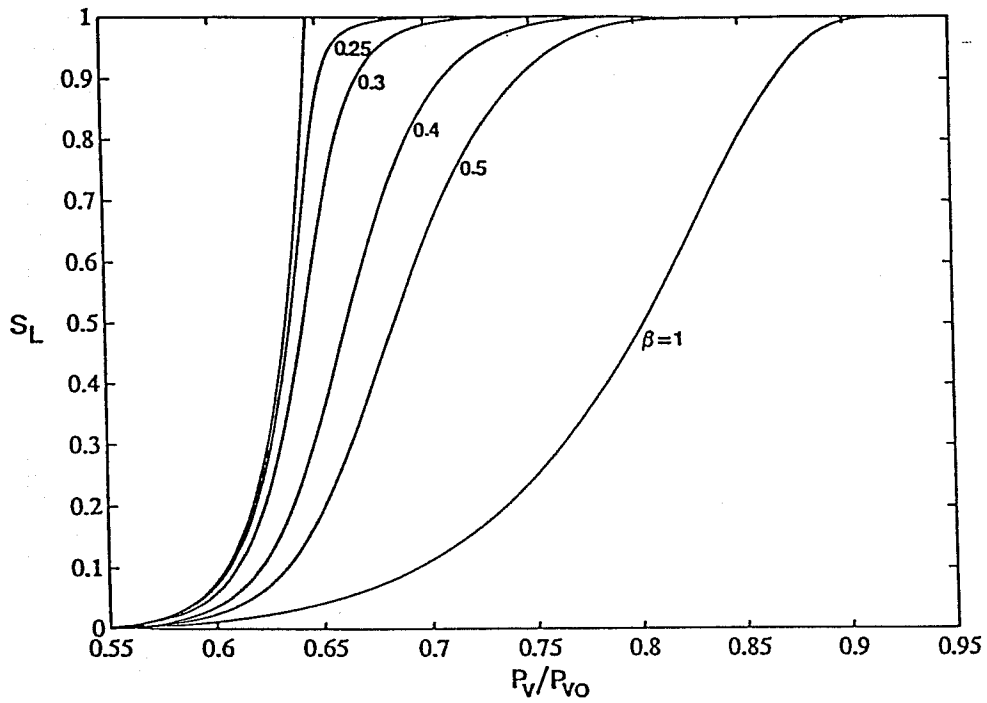


Figure 9. Model Prediction of Primary Desorption Curves for Sorption of Nitrogen for Various Values of β : $Z=4$.

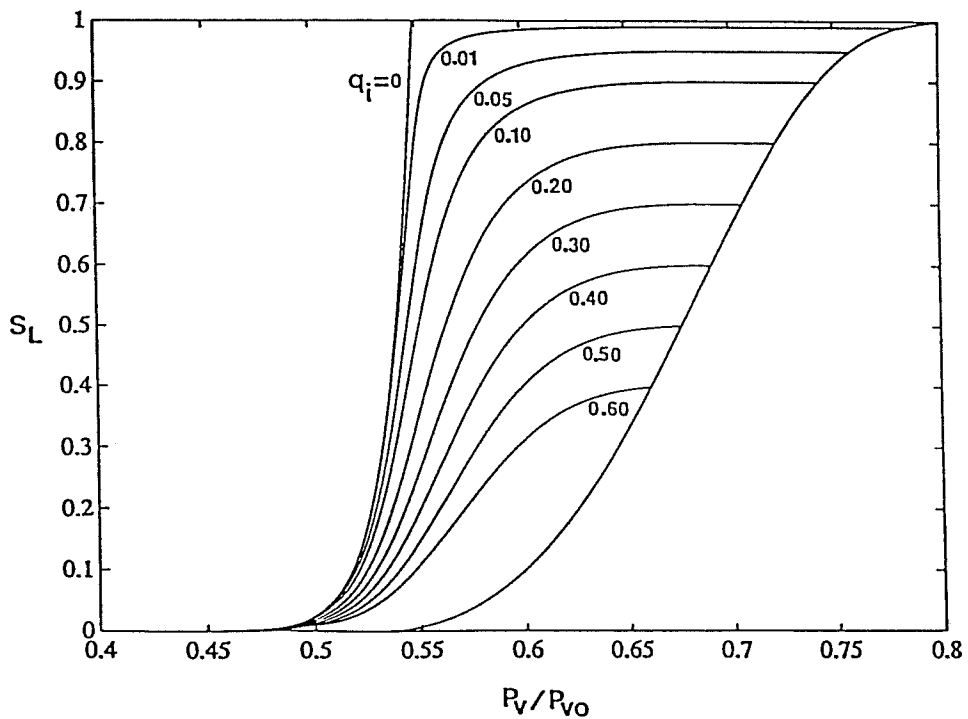


Figure 10. Model Prediction of Secondary Desorption Curves for Sorption of Nitrogen : $Z=4, f_q=0$.

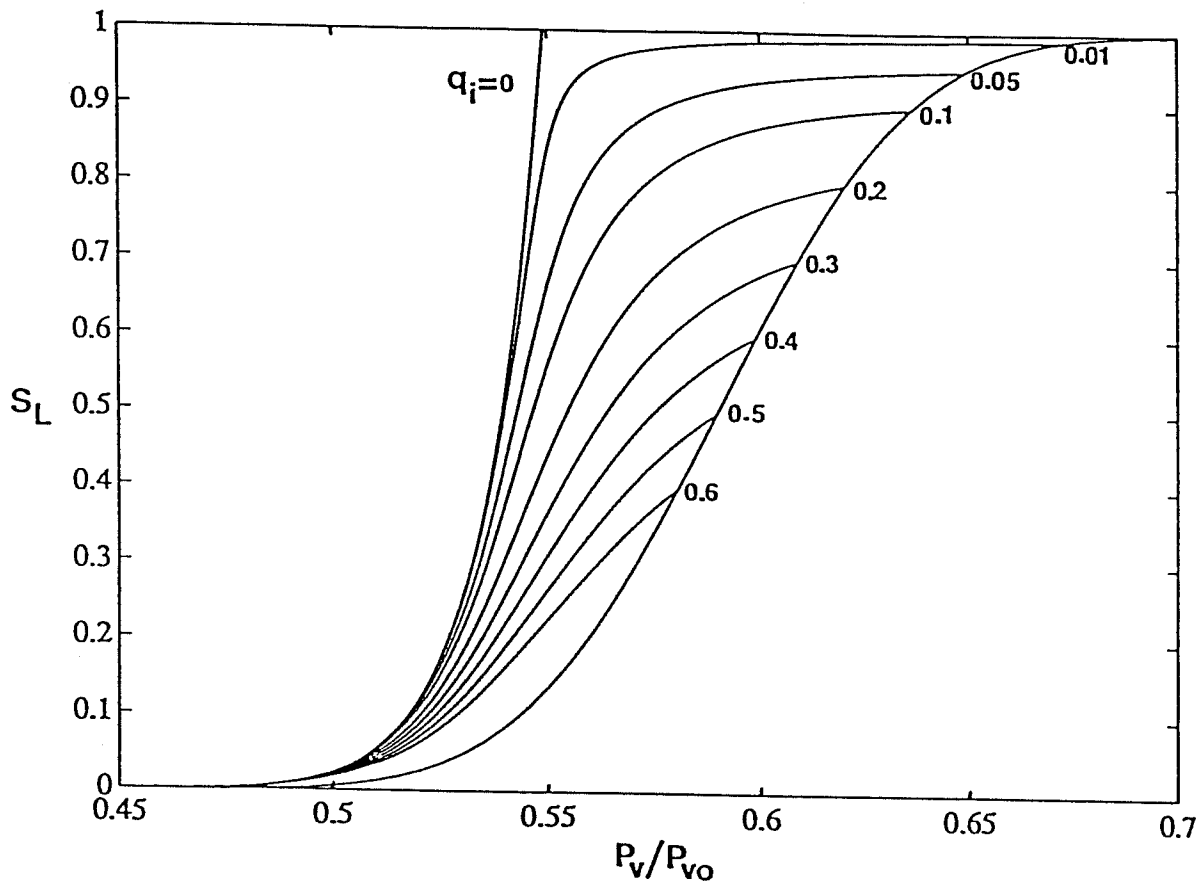


Figure 11. Model Prediction of Secondary Desorption Curves for Sorption of Nitrogen ($q=1-(1-p)^5$): $Z=4$, $f_q=0$.

